

Supplementary Information

Europium doping promoted intermolecular charge transfer in UiO-67-CDC for ultrasensitive turn-on colorimetric detection of an anthrax biomarker

Ming-Cheng Liu,^a Jia-Qi Du,^a Qian Sun,^{*a} and En-qing Gao^b

^a Department of Chemistry, School of Chemistry and Molecular Engineering, East China Normal University, Shanghai 200241, P. R. China

^b Shanghai Key Laboratory of Green Chemistry and Chemical Processes, School of Chemistry and Molecular Engineering, East China Normal University, Shanghai 200062, P. R. China.

Table of contents

S1 Experiment (The synthesis of UiO-67-CDC)

S2 Material characterization(IR,TGA)

S3 Fluorescence spectra of Eu@UiO-67-CDC in different solvents

S4 Standard addition recovery experiment(river water, lake water)

S5 Circulation and stability of Eu@UiO-67-CDC

S6 The fluorescence excitation/emission spectrum of the Eu@UiO-67-CDC and UV-visible absorption spectrum of DPA

S7 XRD of MOF before and after the addition of analytes

S8 Energy level orbital diagram of DPA and ligand

S9 Relevant calculation table

1. Experiment

1.1 Materials and instruments

All reagents used in this study are commercially available and have not undergone post-processing. Zirconium tetrachloride (STREM) and Phloxine B (Macklin) are common reagents. The ligand 9H-carbazole-2,7-dicarboxylic acid (9H-2,7-CDC) was synthesized according to the literature reported by Adam W. Freeman. UV-vis spectra of analytes and Eu@MOF composites were obtained using a GENESYS 10S spectrophotometer with a 200-800 nm scan range. Powder X-ray diffraction patterns (PXRD) were measured using a Bruker D8-ADVANCE diffractometer with Cu-K α radiation. Fluorescence spectra were obtained using an FL980 (Edinburgh) fluorescence spectrophotometer ($\lambda_{\text{ex}} = 320$ nm). ^1H NMR was collected using a Bruker BioSpin GmbH instrument with DMSO-d $_6$ as the deuterated reagent. Infrared spectra were collected using a Nicolet NEXUS 670, ranging from 400 cm^{-1} to 4000 cm^{-1} . Thermogravimetric analysis (TGA) was performed using a Mettler Toledo TGA/SDTA851 e/5FL1100, and Brunauer-Emmett-Teller adsorption and desorption were implemented using Autosorb-IQ.

1.2 Synthesis of UiO-67-CDC

UiO-67-CDC was synthesized using a conventional solvothermal method. 72.8 mg of ZrCl_4 and 79.6 mg of H_2CDC were mixed uniformly with 6.0 mL of DMF. After adding 0.54 mL of glacial acetic acid, the mixture was sonicated for 30 minutes and then sealed in the lining of a stainless steel autoclave. The mixture was heated at 80 $^\circ\text{C}$ for 24 hours. After cooling to room temperature, it was filtered and washed with ethanol three times. The resulting product was dried in a vacuum oven at 60 $^\circ\text{C}$ for 6 hours, yielding 113 mg of a light yellow powder¹.

2. Material characterization

2.1 FT-IR spectra

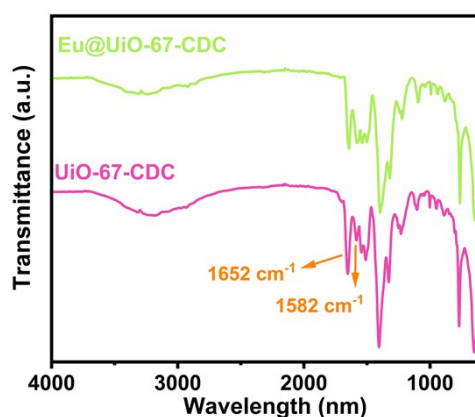


Figure S1 FT-IR spectra of UiO-67-CDC, Eu@UiO-67-CDC.

2.2 Thermogravimetric analysis

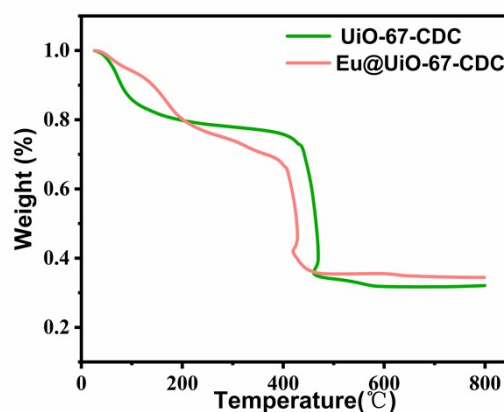


Figure S2 Thermogravimetric analysis of UiO-67-CDC, Eu@UiO-67-CDC.

3. Fluorescence spectra of Eu@UiO-67-CDC in different solvents

Before the experiment, Eu@UiO-67-CDC was immersed in four solvents, methanol, ethanol, DMF, and acetonitrile, to investigate the optimal solvent. The results showed that in DMF solvent, Eu@UiO-67-CDC exhibited significantly higher characteristic peak fluorescence intensity due to DMF's further adequate sensitization of Eu^{3+} . The fluorescence intensity was much higher than the intrinsic luminescence intensity of the MOF, resulting in a robust red color under UV light, which is not conducive to subsequent detection of DPA. As the most common organic solvent, ethanol was suitable for Eu@UiO-67-CDC, as it exhibited a moderate dual-emission fluorescence intensity. Therefore, subsequent tests were conducted in an ethanol system.

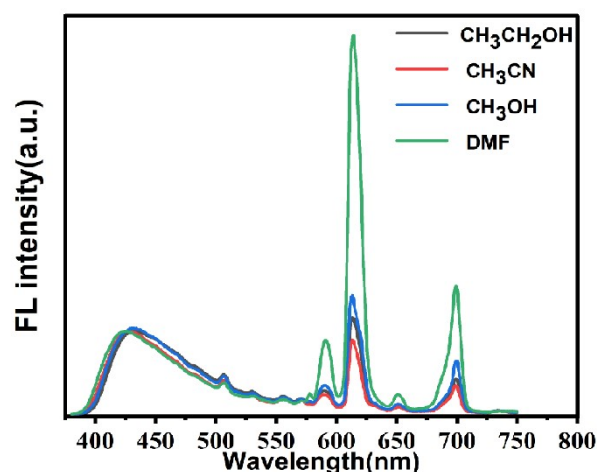


Figure S3 Fluorescence emission spectra of Eu@UiO-67-CDC in different organic solvents.

4. Standard addition recovery experiment (river water, lake water)

The practical application of Eu@UiO-67-CDC was evaluated using river water and lake water samples. After adding a known concentration of DPA (theoretical value) to the actual water sample and detecting the DPA concentration using fluorescence detection with the sensor, the spiked recovery rate can be calculated as follows: spiked recovery rate = (measured value - blank value) / theoretical value. Table S1 shows no DPA was detected in the blank river and lake water samples. The recovery rate of DPA in the actual water samples ranged from 97.43% to 102.37%, with an RSD (n=3) of less than 1.40%. These results indicate that Eu@UiO-67-CDC has good potential for detecting DPA in actual water samples.

Table S1 The Eu@UiO-67-CDC sensor system was used to determine DPA's spiked recovery in lake and river water.

Samples	Added (μM)	Fluorescence method		
		Found (μM)	Recovery (%)	RSDs (%) (n=3)
River water	0	-	-	-
	10	9.98	99.82	1.15
	30	30.19	100.62	1.05
	50	50.91	101.82	1.24
Lake water	0	-	-	-

	10	9.74	97.43	0.92
	30	30.29	100.97	0.98
	50	51.19	102.37	1.40

5. Circulation and stability of Eu@UiO-67-CDC

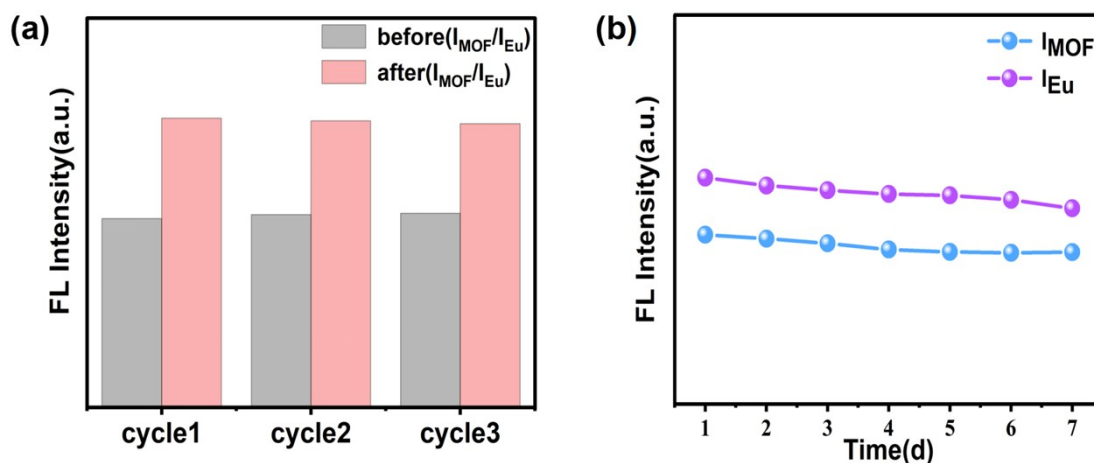


Figure S4 (a) The cyclic experiment diagram of Eu@UiO-67-CDC, (b) the fluorescence intensity diagram of dual emission peaks of Eu@UiO-67-CDC within 7 days.

6. The fluorescence excitation/emission spectrum of the Eu@UiO-67-CDC and UV-visible absorption spectrum of DPA

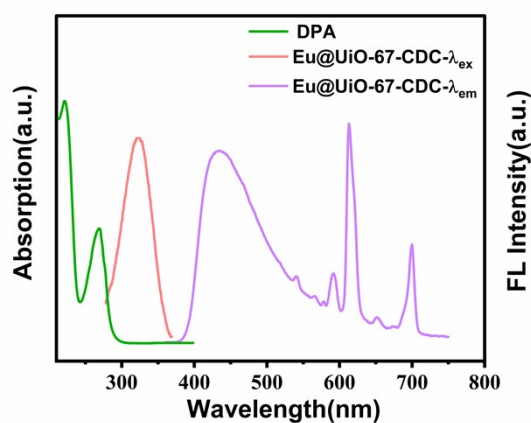


Figure S5 The fluorescence excitation/emission spectrum of the Eu@UiO-67-CDC and UV-visible absorption spectrum of DPA.

7. XRD of MOF before and after the addition of analytes

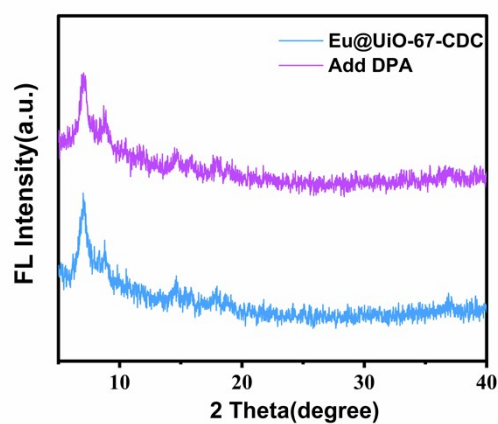


Figure S6 The PXRD patterns of Eu@UiO-67-CDC before and after the addition of DPA.

8. Energy level orbital diagram of DPA and ligand

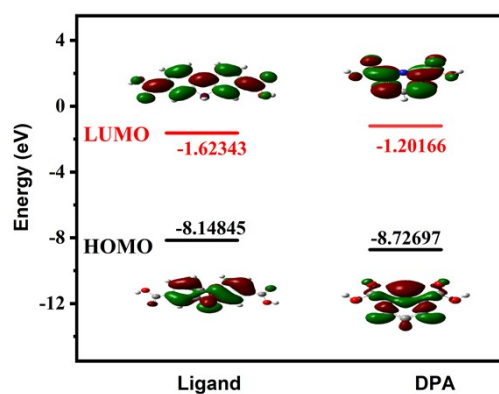


Figure S7 Energy level orbital diagram of the ligand and DPA.

9. Relevant calculation table

Table S2 The molecular size of DPA and $[\text{Eu}(\text{NO}_3)_3(\text{H}_2\text{O})_4] \cdot 2\text{H}_2\text{O}$.

Sample	Size (wt%) ^a		
	a	b	c
DPA	11.210	7.952	3.422
$[\text{Eu}(\text{NO}_3)_3(\text{H}_2\text{O})_4] \cdot 2\text{H}_2\text{O}$	6.705	9.140	11.647

Table S3 The LUMO and HOMO of the ligands CDC^{2-} and DPA.

Sample	DPA	CDC^{2-}
LUMO (eV)	-1.20166	-1.62343

HOMO (eV)	-8.72697	-8.14845
HOMO-LUMO energy band gap(eV)	7.52531	6.52502

Table S4 The S_0 , S_1 , and T_1 energy levels of DPA.

	Energies	Unit
Excited states S_1	-625.05459	Hartree
Ground state S_0	-625.19217	Hartree
Triple excited state T_1	-625.07695	Hartree
S_1-S_0	30194.87993	cm^{-1}
T_1-S_0	25285.70474	cm^{-1}

Table S5 The S_0 , S_1 , and T_1 energy levels of CDC²⁻.

	Energies	Unit
Excited states S_1	-894.23846	Hartree
Ground state S_0	-894.36123	Hartree
Triple excited state T_1	-894.26427	Hartree
S_1-S_0	26945.84218	cm^{-1}
T_1-S_0	21281.21559	cm^{-1}

-
1. A. Das and S. Biswas, *Sensors and Actuators B: Chemical*, 2017, **250**, 121-131.